Arabian Journal of Chemistry (2017) **10**, S230–S235

King Saud University

Arabian Journal of Chemistry

www.ksu.edu.sa
www.sciencedirect.com

ORIGINAL ARTICLE

Antibacterial activity against *Escherichia coli* and characterization of ZnO and ZnO–Al_2O_3 mixed oxide nanoparticles

Ertan Şahin [a], Seyid Javad Musevi [b], Alireza Aslani [c,d,*]

[a] *Department of Chemistry, Faculty of Science, Ataturk University, 25240-Erzurum, Turkey*
[b] *Department of Chemistry, Shahid Beheshti Technical and Vocational University, Urmia, Islamic Republic of Iran*
[c] *Nanobiotechnology Research Center, Baqiyatallah University Medical of Science, Tehran, P.O. Box 19945-581, Islamic Republic of Iran*
[d] *Department of Basic Science, Jundi Shapur University of Technology, Dezful, P.O. Box 64615-334, Islamic Republic of Iran*

Received 29 November 2011; accepted 23 July 2012
Available online 3 August 2012

KEYWORDS

Nanoparticles;
Mixed oxide;
Antibacterial;
Escherichia coli

Abstract In order to achieve better antibacterial water insoluble nanoparticles (Nanoparticles) of ZnO and ZnO–Al_2O_3 were studied. ZnO–Al_2O_3 mixed oxide nanoparticles were produced from a solution containing $Zn(AC)_2 \bullet 2H_2O$ and $AlCl_3$ by Solvothermal method. The calcination process of the ZnO–Al_2O_3 composite nanoparticles brought forth polycrystalline one phase ZnO–Al_2O_3 nanoparticles of 30–50 nm in diameters. ZnO and ZnO–Al_2O_3 were crystallized into würtzite and rock salt structures, respectively. The structural properties of this sample were analyzed by XRD and compared with bulk case of these samples. Antibacterial effectiveness of the ZnO and ZnO–Al_2O_3 nanoparticles were tested against general *Escherichia coli* (*E. coli* ATCC 25922) and *E. coli* O157:H7 by measuring the growth through optical density and digital counting of live–dead cells. Minimum inhibitory concentration values against four representative bacteria along with *E. coli* O157:H7 were also obtained.

1. Introduction

Solvothermal reactions are widely used for the synthesis of solids such as porous, magnetic or electronic compounds as well as catalysts and pigments. The discovery or optimization of new compounds is closely connected with the exploration of the parameter space, which normally comprises of compositional and process parameters. These can range from molar ratios of the starting materials or their order of addition, the pH of the starting mixture and the solvent employed in the synthesis to the reaction time and temperature. While investigations studying one parameter at a time are straightforward, the

* Corresponding author at: Department of Basic Science, Jundi Shapur University of Technology, Dezful, P.O. Box 64615-334, Islamic Republic of Iran. Tel.: +98 914 1261366/916 1161165/641 6268000; fax: +98 641 6260993.
E-mail addresses: Ertan@atauni.edu.tr (E. Şahin), Erkin_musevi@hotmail.com (S.J. Musevi), aslani@jsu.ac.ir, a.aslani110@yahoo.com, ijmet2011@yahoo.com (A. Aslani).
Peer review under responsibility of King Saud University.

Production and hosting by Elsevier

http://dx.doi.org/10.1016/j.arabjc.2012.07.027
1878-5352

simultaneous study of many reaction variables dramatically raises the number of necessary reactions. The serial investigation of such large parameter spaces is impractical and most often infeasible, and high-throughput methods are a more appropriate way (Aslani et al., 2010a,b; Karimi et al., 2010; Aslani, 2011; Aslani and Oroojpour, 2011).

In recent years, controllable synthesis and ordered assembly of nanocrystalline materials is one of the most interesting research areas due to their potential applications in optical and electronic fields, biological labeling and catalysis (Chen et al., 2005; Liu et al., 2001). Their unique properties depend on both the size and the morphology of nanocrystalline materials. A variety of methods have been developed to synthesize nanocrystalline materials with different morphologies. Among them, the traditional method of fabrication of chalcogenide semiconductor is solid synthesis at high temperature ($\geqslant$500 °C), i.e., VLS (vapor–liquid–solid growth), CVT (chemical vapor transport growth) and thermolysis of single source. Nowadays, more attention has been paid to solid synthesis at low temperature, such as electrochemistry, supersonic method, hydrothermal and solvothermal processes. The hydro-solvothermal method is direct, fast and easy than other methods for synthesis of nanomaterials (Aslani et al., 2008, 2009; Aslani and Morsali, 2009). Metal oxide nanoparticles are receiving increasing attention for a large variety of applications. Titanium dioxide and zinc oxide nanoparticles are included in toothpaste, beauty products, sunscreens and textiles. Aluminum oxide having good dielectric and abrasive properties is widely used as an abrasive agent or insulator. The concerns of metal oxide nanoparticles are that because of their chemistry, size, and being not biodegradable, they will rapidly distribute throughout the environment with unknown consequences. Until now little is known about the potential toxicity of metal oxide Nanoparticles in soil and water. Given the well-known toxicity of the ionic forms of many metals, the solubility of metal oxide nanoparticles may require particular attention, and it is important to distinguish effects of Nanoparticles from dissolved metals when assessing the toxicity of metal oxide nanoparticles.

Published studies on the eco toxicity of metal oxide nanoparticles to bacterial species are limited, even though their bactericidal properties have been reported in the biomedical literature (Fu et al., 2005; Duran et al., 2007). One might therefore expect some of these materials to be toxic to microbes in the environment. Zinc oxide (ZnO) nanoparticles seem to disrupt the gram-negative cell membrane structure in *Escherichia coli* (Brayner et al., 2006), and it is proposed that nanoparticles with a positive charge such as cerium oxide could bind the gram-negative cell membrane by electrostatic attraction (Thill et al., 2006). Clearly, the intimate relationship between the physicochemistry of the medium and membrane biology of the microbe is emerging as a key factor in nanoparticles' toxicity to microorganisms. On the other hand the antibacterial properties of some metal oxides have been known for thousands of years and using these properties the ancient Greeks cooked. The adage born with a silver spoon in his mouth, referred to more than just wealth. Currently, the investigation of this phenomenon has gained importance due to the increase of bacterial resistance to antibiotics. *E. coli* inhabit the intestines of humans and other animals. Although most strains of *E. coli* are not pathogenic. *E. coli* O157:H7 produces Shiga-like toxin and causes diarrhea and abdominal cramps (Zhu et al., 2002) and is considered as the most pathogenic strain of *E. coli*. The outbreaks of *E. coli* O157:H7 have been associated with the consumption of foods of animal origin, such as undercooked beef (Ochoa and Harrington, 2005), improperly pasteurized milk (Zhao et al., 2009) or contaminated water (Miles et al., 2009). These bacteria are estimated to cause thousands of food borne illnesses and hundreds of hospitalizations and deaths worldwide each year (Muniesa et al., 2006). It is

Scheme 1 Shows the reaction between $Zn(AC)_2 \bullet 2H_2O$, $AlCl_3$ and sodium hydroxide for the formation of ZnO and ZnO–Al_2O_3 nanoparticles.

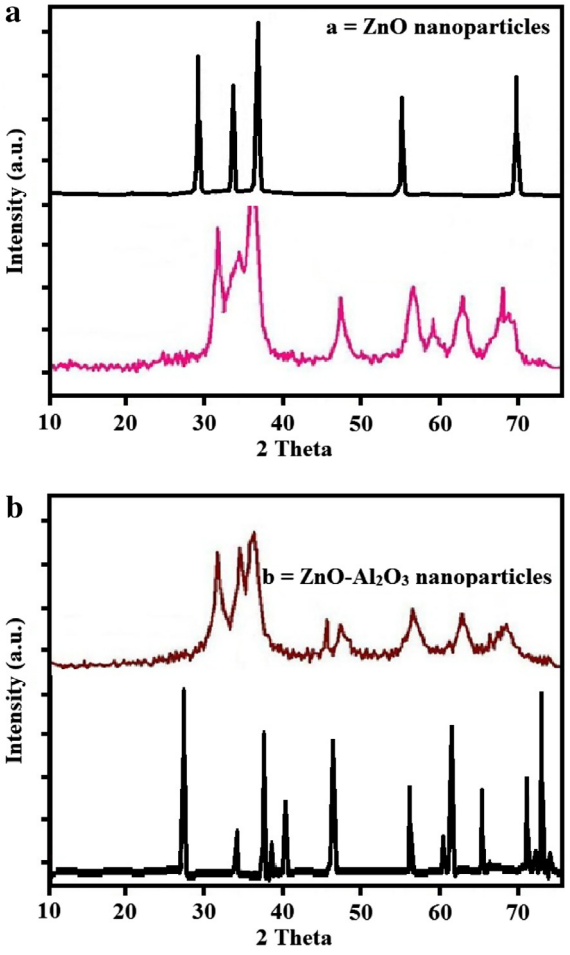

Figure 1 X-ray powder diffraction pattern of (a) ZnO nanoparticles and (b) ZnO–Al_2O_3 nanoparticles.

very important to monitor pathogenic *E. coli* strains and stop their growth by simple and novel means.

Therefore, in developing the route of synthesis, an emphasis was made to control the size of ZnO and ZnO–Al_2O_3 nanoparticles. ZnO and ZnO–Al_2O_3 at bulk size alone in solution easily aggregate resulting in deterioration of their chemical properties and a loss of their antibacterial properties. To solve these problems, we used ZnO and ZnO–Al_2O_3 at nano size. These nanoparticles provide high surface area for surface functionalization, give excellent mechanical strength for supporting other materials, thermal stability and are of low cost.

2. Experimental

ZnO and ZnO–Al_2O_3 nanoparticles were synthesized by methods as reported in references (Aslani et al., 2010a, b; Karimi et al., 2010; Aslani, 2011; Aslani and Oroojpour, 2011). Then XRD structural studies of them were compared to these references. This study show that our synthesized materials are at nano-size. Therefore the synthesized nanoparticles of ZnO and ZnO–Al_2O_3 were used for their antibacterial properties (Maneerung et al., 2008; Aslani et al., 2011a, b).

2.1. Bacterial growth-inhibiting effect based on LB agar plating

The growth-inhibiting effects of ZnO and ZnO–Al_2O_3 nanoparticles were further confirmed by plating on LB agar plates after 24 h of growth at 37 °C in LB broth. The serial dilutions of these mixtures were made in PBS up to 10^{-9} concentration and then plated on LB agar plates.

2.2. Bacterial growth-inhibiting effect in LB broth using turbidity

E. coli strains were cultured on Luria Bertani (LB) agar plates for 18 h at 37 °C before use. Differing concentrations of ZnO and ZnO–Al_2O_3 nanoparticles were prepared in sterilized LB medium in a final volume of 10 ml. The growth of bacteria was monitored with and without ZnO at concentrations of 0.085, 0.85, 8.5, 17, 34, and 42.5 μg/ml, and ZnO–Al_2O_3 nanoparticles at 0.1, 1, 10, and 100 μg/ml. A single colony of *E. coli* was used for inoculating the LB medium containing the nanoparticles as well as a positive control containing only bacteria without ZnO and ZnO–Al_2O_3 nanoparticles. Aliquots were taken every hour up to 9 h and then after 24 h for measurement of the optical density at 620 nm. Samples containing only bac-

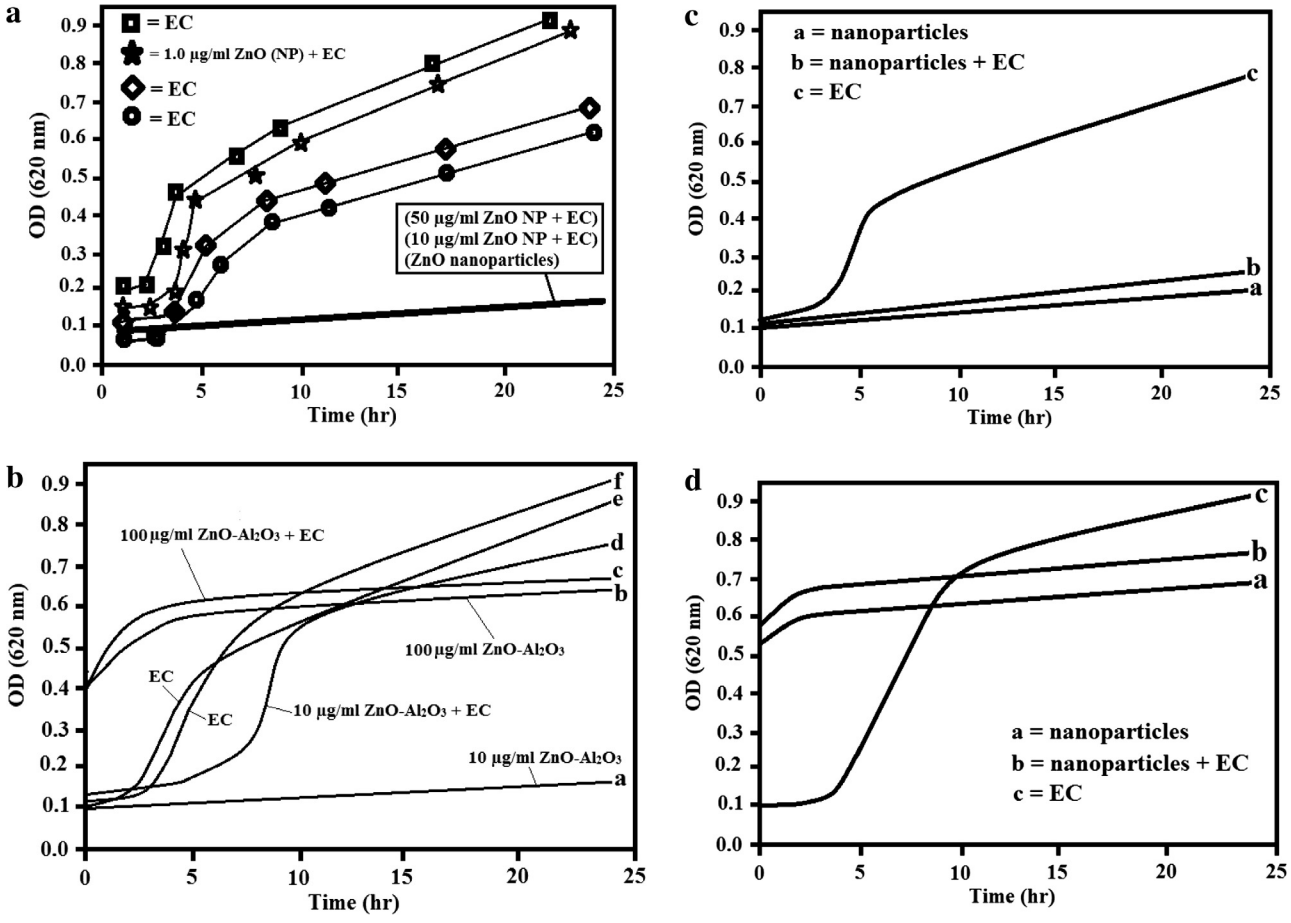

Figure 2 Growth curve of *E. coli* ATCC 25922: (a) in the presence of ZnO nanoparticles at concentrations of 1.0, 10.0 and 50.0 μg/ml with their positive control (only bacteria), respectively and ZnO nanoparticles only as a negative control, (b) in the presence of ZnO–Al_2O_3 nanoparticles at concentrations of 100 and 10 μg/ml, with only bacteria and only ZnO–Al_2O_3 nanoparticles respectively. The growth curve for *E. coli* O157:H7: (c) in the presence of ZnO nanoparticles at concentration of 50.0 μg/ml, only bacteria, and only nanoparticles (d) in the presence of ZnO–Al_2O_3 nanoparticles at concentration of 100 μg/ml, only bacteria, and only ZnO–Al_2O_3 nanoparticles.

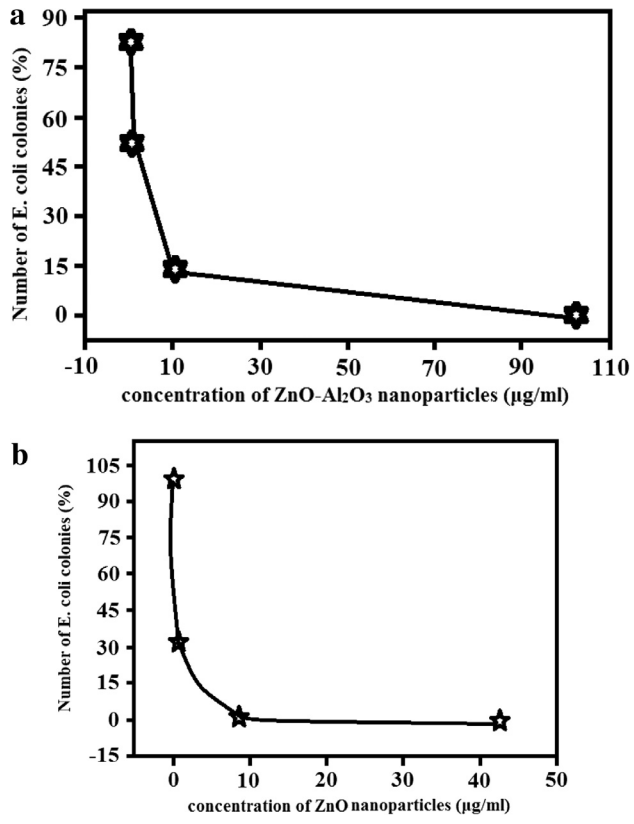

Figure 3 Colonies count of *E. coli* ATCC 25922 expressed as a percentage of the number of colonies grown on silver free LB agar plates, (a) ZnO–Al_2O_3 nanoparticles at 0.1, 1, 10 and 100 µg/ml, (b) colloidal ZnO nanoparticles at 0.1, 1.0, 10.0 and 50.0 µg/ml.

teria were plated as positive controls. The LB broth containing *E. coli* and nanoparticles was diluted based on the growth that was observed though optical density readings. The plates were incubated at 37 °C for 24 h followed by counting the number of colonies on the plate and calculating the increase in colony forming units (cfu)/ml according to following formula (Maneerung et al., 2008).

$$\frac{\text{Viable count at0 h} - \text{Viable count at 24 h}}{\text{Viable count at 0 h}} \times 100 = \text{X}$$

2.3. Bactericidal effect using live–dead cell staining

Experiments were carried out in the presence and absence of silver Nanoparticles to determine the cell viability of *E. coli* and *E. coli* O157:H7 bacteria by using the backlight bacterial viability kit. *E. coli* inoculated LB broth with and without ZnO–Al_2O_3 or ZnO nanoparticles were incubated at 37 °C for 24 h. The samples were centrifuged at 3500°rcf for 10 min in order to pellet the cells and, rinsed 3 times with 1 ml sterile 0.85% KCl solution. After the final rinse, the cells were re-suspended in 1 ml of 0.85% KCl solution and 1 µl of both reagents A and B from the kit was added. The suspension was incubated at RT for 15 min. followed by filtration onto a 25 mm black polycarbonate filter, in order to concentrate the cells. The filter was then placed onto glass microscope slides with cover slips and visualized under a fluorescent microscope using red and green filters for analysis. The dead cells were counted using a red filter while the live cells were counted using the green filter.

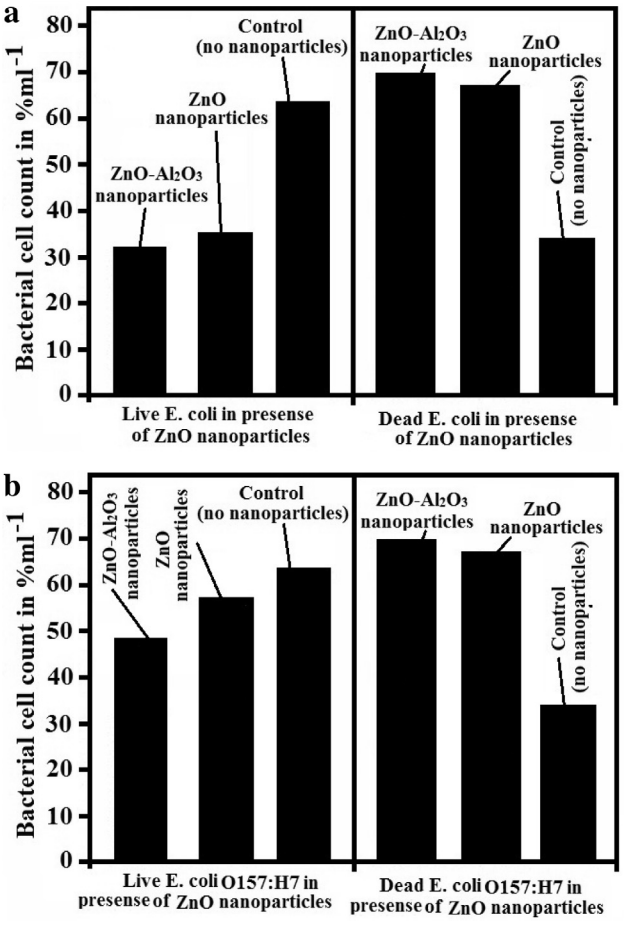

Figure 4 Bar graph of live and dead (a) *E. coli* ATCC 25922 (b) *E. coli* O157:H7 in the presence and absence of ZnO nanoparticles, where bacterial cell counts are expressed as a function of percentage per ml.

Table 1 MIC results of antibacterial property of ZnO and ZnO–Al_2O_3 nanoparticles (µg/mL).

Bacteria	ZnO–Al_2O_3 nanoparticles (µg/mL)	ZnO nanoparticles (µg/mL)
E. coli ATCC 25922	150	50
E. coli O157:H7	150	50
Pseudomonas aeruginosa ATCC 27853	150	50
Salmonella enterica ATCC 19585	150	58
Bacillus cereus	175	58

3. Results and discussions

3.1. Structural study

The reaction between $Zn(AC)_2 \bullet 2H_2O$ and $AlCl_3$ and sodium hydroxide to form ZnO and ZnO–Al_2O_3 nanoparticles has been shown in Scheme 1.

Table 2 MIC results of antibacterial property of ZnO and $ZnO–Al_2O_3$ at bulk size (mg/mL).

Bacteria	ZnO powders at bulk size (mg/mL)	ZnO/Al_2O_3 powders at bulk size (mg/mL)
E. coli ATCC 25922	512	250
E. coli O157:H7	512	250
Pseudomonas aeruginosa ATCC 27853	512	250
Salmonella enterica ATCC 19585	512	275
Bacillus cereus	575	275

In the XRD spectra of ZnO and $ZnO–Al_2O_3$ nanoparticles we can observe the formation of well crystalline hexagonal structure. On the other hand XRD spectra show that there was no other phase corresponding to Al_2O_3. Sharp diffraction peaks shown in Fig. 1a and b indicate the good crystalline structure of ZnO and $ZnO–Al_2O_3$ nanoparticles. No characteristic peak related to any impurity was observed. The broadening of the peaks indicated that the particles were of nanometer scale.

3.2. Antibacterial studies

In order to test the antibacterial effectiveness of these nanoparticles against general *E. coli* and *E. coli* O157:H7 the optical density (OD) was measured in LB broth in the presence and absence of nanoparticles. A level of 10.0 or 50.0 μg/ml of ZnO nanoparticles totally inhibited the growth of the general strain of *E. coli* throughout the 24 h period of incubation (Fig. 2a). Limited inhibition was observed at 10.0 μg/ml. The $ZnO–Al_2O_3$ nanoparticles at 10 μg/ml inhibited the growth of the general *E. coli* strain up to 6 h while 100 μg/ml was effective throughout the 24 h incubation and totally prevented growth (Fig. 2b). As is noted 100 μg/ml $ZnO–Al_2O_3$ nanoparticles' control did result in a high initial turbidity but there was no apparent change over time indicating inhibition of bacterial growth. In tests against *E. coli* O157:H7, the higher concentration of ZnO nanoparticles (50.0 μg/ml) and $ZnO–Al_2O_3$ nanoparticles (100 μg/ml) also inhibited the growth up to 24 h (Fig. 2c and d, respectively).

Plate counts were also used to monitor growth of the general strain of *E. coli* at the end of the 24 h incubation. The inhibitory effects, observed using turbidity were confirmed using plate counts. It should be pointed out that the samples with nanoparticles were diluted prior to plating; however, the nanoparticles were still present in the plates and thus likely influenced growth on the plates. Concentrations of 5 and 10 μg/ml of $ZnO–Al_2O_3$ and 10.0 μg/ml ZnO nanoparticles reduced growth of *E. coli* on the plates, but no growth was observed at 100 μg/ml of $ZnO–Al_2O_3$ and at 50.0 μg/ml of ZnO nanoparticles (Fig. 3a and b, respectively). These results confirm that the synthesized $ZnO–Al_2O_3$ nanoparticles have antibacterial effectiveness similar to ZnO nanoparticles. The digital counting of live vs. dead bacterial cells was expressed as the function of percentage and results are the mean of some images. In the presence of 100 μg/ml of $ZnO–Al_2O_3$ nanoparticles 82% of the general strain were killed whereas 72% of *E. coli* O157:H7 were killed (Fig. 4a and b). 10.0 μg/ml ZnO nanoparticles showed similar results with 78% death of the general strain and 68% death of *E. coli* O157:H7.

For demonstrating the antibacterial activity of ZnO and ZnO/Al_2O_3 powders at bulk size, *E. coli* and *E. coli* O157:H7 were selected as the bacteria, respectively. For bulk ZnO and bulk ZnO/Al_2O_3 powders, MIC values obtained from the broth dilution test for *E. coli* and *E. coli* O157:H7 aurous were 512 and 250 mg/mL, respectively and depended on the size of ZnO and ZnO/Al_2O_3 powders. However, these values were not better than ZnO and ZnO/Al_2O_3 nanopowders. Because there is no recommended standard materials for testing the inhibitory activities of inorganic antibacterial agents. But the use of nanoparticles of ZnO and ZnO/Al_2O_3 gives better results for antibacterial activity of these compounds. On the other hand the concentration of ZnO and ZnO/Al_2O_3 powders that were used in this work for comparison of the size effect on antibacterial activity indicates that the nanoparticles of ZnO and ZnO/Al_2O_3 powders give good result from ZnO and ZnO/Al_2O_3 powders at bulk size (see Table. 2.).

4. Conclusion

In conclusion, we could develop a simple low-temperature solvothermal method to synthesize single crystalline, hexagonal ZnO and $ZnO–Al_2O_3$ nanoparticles with different ratio. Though several low-temperature chemical or solvothermal syntheses of ZnO and $ZnO–Al_2O_3$ nanoparticles have been reported our low-temperature synthesis method allows synthesizing ZnO and $ZnO–Al_2O_3$ nanostructures of several morphologies in a controlled manner.

The OD graph and agar plate readings of well dispersed ZnO nanoparticles at 50.0 μg/ml and $ZnO–Al_2O_3$ nanoparticles at 100 μg/ml show almost similar antibacterial effectiveness in LB broth against *E. coli* ATCC 25922 and *E. coli* O157:H7. The mechanism of antibacterial property of ZnO nanoparticles has been well established by free-radical generation from ZnO nanoparticles using electron spin resonance spectroscopy. In the presence of 10 μg/ml of $ZnO–Al_2O_3$ nanoparticles, growth of both *E. coli* ATCC 25922 and *E. coli* O157:H7 was inhibited, and at 100 μg/ml, the bacteria did not grow even after 24 h. At $ZnO–Al_2O_3$ nanoparticles concentration of 100 μg/ml 82% of the general *E. coli* and 72% of *E. coli* O157H7 were killed.

Further, antibacterial properties of $ZnO–Al_2O_3$ and ZnO nanoparticles were shown with both Gram negative and positive bacteria. MIC values show that 150 μg/ml $ZnO–Al_2O_3$ nanoparticles and 60 μg/ml ZnO nanoparticles were sufficient for Gram negative bacteria (*E. coli* ATCC25922, *E. coli* O157:H7, Pseudomonas aeruginosa ATCC27853, Salmonella enterica ATCC19585 (50.0 μg/ml; ZnO nanoparticles) while, 170 μg/ml $ZnO–Al_2O_3$ nanoparticles and 50.0 μg/ml ZnO nanoparticles were required for the Gram positive bacteria (Bacillus cereus) (Table. 1). This difference could be due to the difference in bacterial concentration as well as the type of strain used.

Acknowledgements

Supporting of this investigation by Jundi Shapur University of Technology (Dezful, Islamic Republic of Iran), Baqiyatallah

University Medical of Science (Tehran, Islamic Republic of Iran) and Kimya Javid Company, Gitipasand industrial company, (Isfahan. Islamic Republic of Iran) is gratefully acknowledged. This work proffer to "Dr. Masoud Alimohammadi, Dr. Majid Shariyari, Mostafa Ahmadi Roshan, Dariush Razaeinejad, Reza Ghashghaei and Dr. Hassan Tehrani Moghaddam".

References

Aslani, A., Shamili, A.R.B., Barzegar, S., 2010a. Solvothermal synthesis, characterization and optical properties of ZnO and ZnO–Al2O3 mixed oxide nanoparticles.. Phys. B Phys. Condens. Matter 405, 3585–3589.

Aslani, A., Shamili, A.R.B., Kaviani, K., 2010b. Sonochemical synthesis, characterization and optical analysis of some metal oxide nanoparticles (MO-NP; M = Ni, Zn and Mn).. Phys. B Phys. Condens. Matter 405, 3972–3976.

Karimi, R.R., Shamili, A.R.B., Aslani, A., Kaviani, K., 2010. Sonochemical synthesis, characterization and thermal and optical analysis of CuO nanoparticles.. Phys. B Phys. Condens. Matter 405, 3096–3100.

Aslani, A., 2011. Controlling the morphology and size of CuO nanostructures with synthesis by solvo/hydrothermal method without any additives.. Phys. B Phys. Condens. Matter 406, 150–154.

Aslani, A., Oroojpour, V., 2011. CO gas sensing of CuO nanostructures, synthesized by an assisted solvothermal wet chemical route.. Phys. B Phys. Condens. Matter 406, 144–149.

Chen, H.F., Clarkson, B.H., Sun, K., Mansfield, J.F., 2005. Self-assembly of synthetic hydroxyapatite nanorods into an enamel prism-like structure.. Colloid Interf. Sci. 288, 97–103.

Liu, Y., Zhan, J., Ren, M., Tang, K., Yu, W., Qian, Y., 2001. Hydrothermal synthesis of square thin flake CdS by using surfactants and thiocarbohydrate.. Mater. Res. Bull. 36, 1231–1236.

Aslani, A., Morsali, A., Yilmaz, V.T., Kazak, C. 2009. Hydrothermal and sonochemical synthesis of a nano-sized 2D lead(II) coordination polymer: A precursor for nano-structured PbO and PbBr2. 929, 187–192.

Aslani, A., Morsali, A., 2009. Sonochemical synthesis of nano-sized metal-organic lead(II) polymer: A precursor for the preparation of nano-structured lead(II) iodide and lead(II) oxide.. Inorg. Chim. Acta 362, 5012–5016.

Aslani, A., Morsali, A., Zeller, M., 2008. Nano-structures of two new lead(II) coordination polymers: New precursors for preparation of PbS nano-structures.. Solid State Sci. 10, 1591–1597.

Fu, G., Vary, P.S., Lin, C.T., 2005. Conformational sampling of peptides in cellular environments.. J. Phys. Chem B. 109, 89–98.

Duran, N., Marcato, P.D., De Souza, G.I.H., Alves, O.L., Esposito, E., 2007. Use of nanoparticles in soil-Water bioremediation processes.. J. Biomed. Nanotech. 3, 203–208.

Brayner, R., Ferrari-Iliou, R., Brivois, N., Djediat, S., Benedetti, M.F., Fievet, F., 2006. Toxicological impact studies based on Escherichia coli bacteria in ultrafine ZnO nanoparticles colloidal medium.. Nano Lett. 6, 866–870.

Thill, A., Zeyons, O., Spalla, O., Chauvat, F., Rose, J., Auffan, M., 2006. Occurrence and origin of estrogenic isoflavones in Swiss river waters.. Environ. Sci. Technol. 40, 6151–6157.

Zhu, Q., Li, L., Guo, Z., Yang, R., 2002. Identification of Shiga-like toxin Escherichia coli isolated from children with diarrhea by polymerase chain reaction.. Chin. Med. J. 115, 815–818.

Ochoa, M.L., Harrington, P.B., 2005. Immunomagnetic isolation of enterohemorrhagic Escherichia coli O157:H7 from ground beef and identification by matrix-assisted laser desorption/ionization time-of-flight mass spectrometry and database searches.. Anal. Chem. 77, 5258–5268.

Zhao, Y., Ye, M., Chao, Q., Jia, N., Ge, Y., Shen, H., 2009. Simultaneous detection of multifood-borne pathogenic bacteria based on functionalized quantum dots coupled with immunomagnetic separation in food samples.. J. Agric. Food Chem. 57, 517–524.

Miles, S.L., Gerba, C.P., Pepper, I.L., Reynolds, K.A., 2009. Point-of-use drinking water devices for assessing microbial contamination in finished water and distribution systems.. Environ. Sci. Technol. 43, 1425–1429.

Muniesa, M., Jofre, J., Garcia-Aljaro, C., Blanch, A.R., 2006. Occurrence of escherichia coli O157; H7, and other enterohemorrhagic Escherichia coli in the environment.. Environ. Sci. Technol. 40, 7141–7149.

Maneerung, T., Tokura, S., Rujirvanit, R., 2008. Impregnation of silver nanoparticles into bacterial cellulose for antimicrobial wound dressing.. Carbohydr. Poly. 72, 43–51.

Aslani, A., Arefi, M.R., Babapoor, A., Amiri, A., Shuraki, K.B., 2011a. Solvothermal synthesis, characterization and optical properties of ZnO, ZnO–MgO and ZnO–NiO, mixed oxide nanoparticles.. Appl. Surf. Sci. 257, 4885–4889.

Aslani, A., Oroojpour, V., Fallahi, M., 2011b. Sonochemical synthesis, size controlling and gas sensing properties of NiO nanoparticles.. Appl. Surf. Sci. 257, 4056–4061.